Vector Control of Induction Motor without Shaft Encoder

Tsugutoshi Ohtani, *Member, IEEE,* Noriyuki Takada, and Koji Tanaka

Abstract—**A new method of induction motor drive, which requires no shaft encoder, is presented. This system has both torque and speed controls that are performed by vector control. The proposed vector-control scheme is based on a rotor-flux speed control, which is performed by torque-producing current and rotor flux, derived from the stator voltages and currents. If it is possible to obtain both precise torque-producing current and rotor flux, this system will have a good torque and speed performance because of the direct control of the torque and rotor flux. The characteristics of the vector control employing stator voltages and currents usually deteriorate as the speed gets lower because the calculated rotor flux depends on the stator resistance, and it is difficult to calculate rotor flux at standstill. In this new system, the rotor-flux estimator is improved to reduce the stator-resistance influence and to make it possible to calculate rotor flux at standstill.**

Nomenclature

[Variables in a $d-q$ frame rotating together with rotor flux]

V_{d1}, V_{q1}	d, q component of stator voltage
$\boldsymbol{V}_1$	vector of stator voltage ($= V_{d1} + jV_{q1}$)
I_{d1}, I_{q1}	$d-q$ component of stator current
I_{d2}, I_{q2}	$d-q$ component of rotor current
$\boldsymbol{I}_1$	vector of stator current ($= I_{d1} + jI_{q1}$)
Ψ_d, Ψ_q	$d-q$ component of rotor flux
$\boldsymbol{\Psi}$	vector of rotor flux ($= \Psi_d + j\Psi_q$)
γ^*	stator current phase to rotor-flux in commands $\{= \tan^{-1}(I_{q1}^*/I_{d1}^*)\}$
γ	stator current phase to rotor-flux in actual values

[Variables in an $\alpha-\beta$ stationary frame]

v_α, v_β	α, β phase of stator voltage
$\boldsymbol{v}_1$	vector of stator voltage ($= v_\alpha + jv_\beta$)
$\boldsymbol{e}$	rotor-induced voltage translated into stator
i_α, i_β	α, β phase of stator current
$\boldsymbol{i}_1$	vector of stator current ($= i_\alpha + ji_\beta$)
ψ_α, ψ_β	α, β phase of rotor flux translated into stator
$\boldsymbol{\psi}$	vector of rotor flux ($= \psi_\alpha + j\psi_\beta$)
i_{d1}	d component of stator current $[= I_{d1}\epsilon^{j(\omega t+\rho)}]$
i_{q1}	q component of stator current $[= I_{q1}\epsilon^{j(\omega t+\rho+\pi/2)}]$

[Velocities, electrical angle, and torques]

ω	angular speed of $d-q$ reference frame
ω_s	slip angular speed
ω_n	rotor angular speed
τ_e, τ	electromagnetic, mechanical torque
θ	angle of $d-q$ frame in stator reference frame ($= \omega t$)

[Motor parameters]

L_1	stator self-inductance ($= M + l_1$)
L_2	rotor self-inductance ($= M + l_2$)
M	mutual inductance
l	total leakage inductance ($= L_1(1 - M^2/L_1L_2)$)
l_1, l_2	stator, rotor-leakage inductance
R_1, R_2	stator, rotor resistance
ΔR_1	deviation of stator resistance ($= R - R_1^*$)
Δr_1	deviation of stator resistance per unit ($= \Delta R_1/R_1^*$)
Δl	deviation of leakage inductance ($= l - l^*$)
$\Delta\sigma$	deviation of leakage inductance per unit ($= \Delta l/M^*$)
T_2	time constant of rotor circuit ($= L_2/R_2$)

[Lag-circuit parameters]

T_L	time constant of lag circuit
γ_c	phase lag due to lag circuit ($= \tan^{-1}\omega T_L$)
δ_c	phase lead due to lag circuit ($= \tan^{-1}(1/\omega T_L)$)
δ_u	phase error of rotor flux in conventional method
δ_p	phase error of rotor flux in proposed method
F_L	function of lag circuit $[= (1 + (\omega T_L)^2)^{-1/2} \cdot \epsilon^{-j\gamma_c}]$

[Subscripts]

p	derivative operator ($= d/dt$)
1, 2	symbol of stator and rotor, respectively
*, c	command or setting value and calculated value, respectively

Paper IPCSD 91-45, approved by the Industrial Drives Committee of the IEEE Industry Applications Society for presentation at the 1989 Industry Applications Society Annual Meeting, San Diego, CA, October 1-5.

The authors are with the Yaskawa Electric Mfg. Co., Ltd., Fukuoka, Japan.

IEEE Log Number 9103278.

I. Introduction

In recent years, commercial applications of vector-controlled induction motor drives have greatly increased, including machine tools, steel and paper machines, and a wide variety of different applications used mainly in Japan [2]. The conventional method of vector control has been

0093-9994/92$03.00

slip-frequency control. This method reduces the structural features of squirrel-cage induction motors and restricts the applications because it requires a speed sensor. Lately, the method of vector control without shaft encoder has been developed, employing the flux calculated from the stator voltages and currents [3]–[8]. However, the problems for practical use, such as a low-speed behavior, have rarely been found in the above papers.

This paper describes the high-performance drive that can be obtained from a vector-control drive and an induction motor without shaft encoder, where both torque and speed can be precisely controlled over a wide speed and load range. This control scheme is based on the vector control in which the rotor-flux speed is controlled with the torque-producing current and the rotor flux calculated from stator voltages and currents.

In the conventional method, the characteristics of the system have deteriorated in the low-speed range because the calculated rotor flux depends on the stator resistance and calculating the rotor flux does not work at standstill. In the new system, the rotor-flux estimator has been improved to reduce the stator-resistance influence and to make it possible to calculate the rotor flux at standstill.

In the proposed rotor-flux estimator, a lag circuit is employed, to which both the motor-induced voltage and the rotor-flux command are imposed, and therefore it is possible to calculate even a low frequency down to standstill. In addition, selecting the rotor-flux estimator parameter to set the same time constant to the lag circuit as that of the rotor-circuit is considered to reduce the influence of stator resistance. Consequently, the proposed system can be controlled precisely over a wide speed and load range. These features are verified by the theoretical examination, the experimental results, and the application for printing presses.

II. Principles of Proposed System

The proposed system is constituted of torque and speed controls that are based on vector control using stator voltages and currents. The method of vector control for induction motors has been derived from the basic equations of induction motors. Because a three-phase induction motor can be theoretically converted to an equivalent two-phase motor, a two-phase two-pole motor is assumed to simplify the analysis process.

The voltage equation of the induction motor is given by (1), in a $(d-q)$ reference frame rotating together with the rotor flux:

$$\begin{bmatrix} V_{d1} \\ V_{q1} \\ 0 \\ 0 \end{bmatrix} = \begin{bmatrix} R_1 + L_1 p & -L_1\omega & Mp & -M\omega \\ L_1\omega & R_1 + L_1 p & M\omega & Mp \\ L_2 p & -L_2\omega_s & R_2 + L_2 p & -L_2\omega_s \\ L_2\omega_s & L_2 p & L_2\omega_s & R_2 + L_2 p \end{bmatrix} \begin{bmatrix} I_{d1} \\ I_{q1} \\ I_{d2} \\ I_{q2} \end{bmatrix} \tag{1}$$

where

ω rotor-flux angular speed
ω_n rotor angular speed
ω_s slip angular speed $(= \omega - \omega_n)$.

The equivalent circuit to represent motor parameters is shown in Fig. 1.

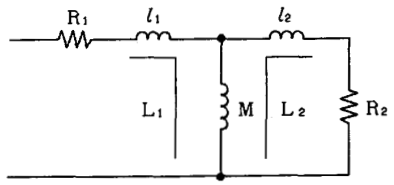

Fig. 1. Equivalent circuit for induction motor.

Assuming the rotor-flux components to be $\Psi_d = MI_{d1} + L_2 I_{d2}$, $\Psi_q = MI_{q1} + L_2 I_{q2}$, and the total leakage inductance as $l = L_1(1 - M^2/L_1 L_2)$, the basic equation can be expressed as follows:

$$\left.\begin{aligned} V_{d1} &= (R_1 + lp) I_{d1} - \omega l I_{q1} + p\Psi_d - \omega\Psi_q \\ V_{q1} &= (R_1 + lp) I_{q1} + \omega l I_{d1} + p\Psi_q + \omega\Psi_d \\ 0 &= R_2 I_{d2} + p\Psi_d - \omega_s\Psi_q \\ 0 &= R_2 I_{q2} + p\Psi_q + \omega_s\Psi_d \end{aligned}\right\} \tag{2}$$

and electromagnetic torque τ_e can be expressed as

$$\tau_e = \Psi_d I_{q2} - \Psi_q I_{d2}. \tag{3}$$

A significant simplification can be achieved if the d axis coincides with the resultant rotor-flux Ψ axis, i.e., $\Psi_d = \Psi$, $\Psi_q = 0$. Therefore, electromagnetic torque τ_e, rotor angular speed ω_n, slip angular speed ω_s, and rotor-flux Ψ can be written as follows:

$$\begin{aligned} \tau_e &= \Psi I_{q2} \\ &= -\frac{M}{L_2}\Psi I_{q1} \end{aligned} \tag{4}$$

$$\omega_n = \omega - \omega_s \tag{5}$$

$$\omega_s = \frac{M}{L_2} \cdot \frac{R_2 I_{q1}}{\Psi} \tag{6}$$

$$\Psi = \frac{MI_{d1}}{1 + T_2 p} \tag{7}$$

where

$$T_2 = \frac{L_2}{R_2}.$$

When Ψ is constant, (7) is rewritten in (8):

$$\Psi = MI_{d1}. \tag{8}$$

In other words, both electromagnetic torque τ_e and rotor angular speed ω_n can be represented, with only rotor-flux Ψ and torque-producing current I_{q1}, which can be calculated from the stator variables.

The scheme of the proposed method is based on the control of the rotor-flux speed, by which torque-producing current I_{q1} is controlled to coincide with its command I_{q1}^*. Fig. 2

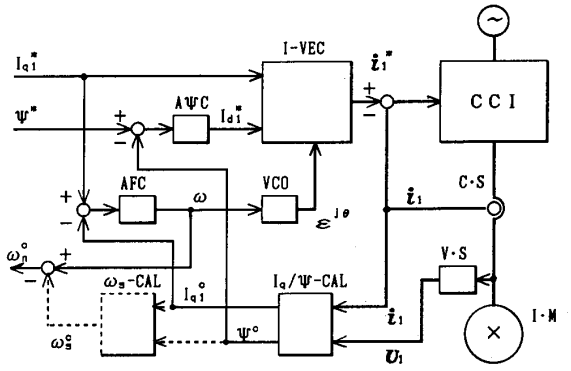

Fig. 2. Concept of proposed vector-control method. I · M = induction motor; CCI = current-controlled con inverter; I-VEC = calculator of current vector; VCO = voltage-controlled oscillator; I_q/Ψ – CAL = calculator of torque-producing current and flux; ω_s – CAL = calculator of slip angular frequency; AFC = frequency controller; AΨC = flux controller; C · S = current sensor; V · S = voltage sensor.

shows the configuration of the proposed method, which is composed of a current-controlled inverter, a squirrel-cage induction motor, and the controller that contains several functions.

Stator current command I_1^* is given with rotor-flux current command I_{d1}^* and torque-producing current command I_{q1}^* and it is shown in (9):

$$I_1^* = I_1^* \epsilon^{j\gamma^*} \tag{9}$$

where

$$I_1^* = \left(I_{d1}^{*2} + I_{q1}^{*2}\right)^{1/2} \qquad \gamma^* = \tan^{-1}\left(I_{q1}^*/I_{d1}^*\right).$$

Accordingly, stator current vector I_1^* is translated into i_1^* in a stationary reference frame:

$$i_1^* = I_1^* \epsilon^{j(\theta+\gamma^*+\rho)} \tag{10}$$

where $\theta + \rho$ is the angle of the d axis to the α axis, $\theta = \omega t$, and ρ is the arbitrary angle at $t = 0$. Then, i_1^* is translated into current commands i_α, i_β in an α, β stationary reference frame.

Assuming phase γ of I_1 to actual rotor-flux Ψ, whereas I_{q1} and γ are represented in (11), and (12), I_{q1} can be controlled with ω_s:

$$I_{q1} = I_1 \sin\gamma \tag{11}$$

$$\gamma = \tan^{-1}\left(\omega_s T_2\right). \tag{12}$$

Decoupling the torque-producing current from the rotor flux can be achieved if I_{q1} agrees with I_{q1}^* to be $\Psi_q = 0$. As a result, stator current phase γ agrees with its setting value γ^* if stator current I_1 can be controlled according to its command I_1^* and the motor parameters coincide with its setting values.

On the other hand, the estimated speed signal ω_n^c is calculated from the rotor flux angular speed ω and the slip angular speed command ω_s with the following equation:

$$\omega_n^c = \omega - \omega_s^c \tag{13}$$

where

$$\omega_s^c = \left(1/T_2^*\right) \cdot \left(I_{q1}^*/I_{d1}^*\right).$$

The speed control can be performed using estimated speed signal ω_n^c. This system will have an exceptional torque control because of the direct control of the torque-producing current if both torque-producing current and the rotor flux can be precisely obtained.

III. Strategies for Realizing the Proposed Method

Availability of the proposed method depends on the characteristics of the torque-producing current and the rotor flux. We examined both the torque-producing current and the rotor flux, which are calculated from the stator voltages and currents.

Torque-producing current I_{q1} and electromagnetic torque τ_e are represented by flux ψ_α, ψ_β and stator current i_α, i_β in an α, β stationary reference frame:

$$\tau_e = -\frac{M}{L_2}\left(\psi_\alpha i_\beta - \psi_\beta i_\alpha\right) \tag{14}$$

$$I_{q1} = -\frac{\psi_\alpha i_\beta - \psi\beta i_\alpha}{\left(\psi_\alpha^2 + \psi_\beta^2\right)^{1/2}} \tag{15}$$

where

$$\psi_\alpha = \Psi\cos\left(\omega t + \rho\right), \psi_\beta = \Psi\sin\left(\omega t + \rho\right)$$

$$i_\alpha = I_1\cos\left(\omega t + \gamma^* + \rho\right)$$

$$i_\beta = I_1\sin\left(\omega t + \gamma^* + \rho\right).$$

Flux ψ_α, ψ_β are represented in (16):

$$\psi_\alpha = \int\left(v_\alpha - R_1 i_\alpha\right)dt - li_\alpha$$

$$\psi_\beta = \int\left(v_\beta - R_1 i_\beta\right)dt - li_\beta \tag{16}$$

where v_α and v_β are the stator voltages in an α, β stationary reference frame.

There are two problems with respect to the calculated rotor-flux vector as follows:

1) *Integrating operation by which the rotor induced voltage is converted into the rotor flux.* Calculated rotor flux does not work so that it is unstable in initial operation, as motor speed approaches zero.
2) *Dependence of motor parameters, such as stator-resistance thermal variation and saturation of inductance parameters.* Particularly, stator-resistance variation causes the calculated rotor flux to vary and lead to torque variation in a low-speed range.

The proposed rotor-flux estimator is shown in Fig. 3 and composed of two lag circuits. Rotor-induced voltage e is imposed to the lag circuit: $T_L/(1 + T_L p)$, and rotor-flux command ψ^* is imposed to the other lag circuit: $1/(1 + T_L p)$, and the addition of them becomes the estimated value of the rotor flux.

Calculated rotor-induced voltage e^c is obtained by subtracting the stator resistance and the total leakage reactance-

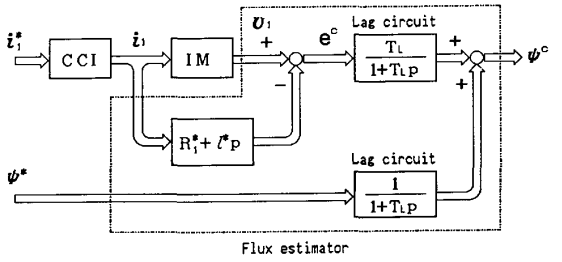

Fig. 3. Proposed rotor-flux estimator.

drop voltage from the stator voltage

$$\begin{aligned} \boldsymbol{e}^c &= \boldsymbol{v}_1 - (R_1^* + l^* p)\boldsymbol{i}_1 \\ &= \boldsymbol{e} + (\Delta R_1 + \Delta l p)\boldsymbol{i}_1 \end{aligned} \tag{17}$$

where

$$\boldsymbol{v}_1 = v_\alpha + jv_\beta \qquad \boldsymbol{i}_1 = \boldsymbol{i}_\alpha + j\boldsymbol{i}_\beta$$

R_1^*, l^* = setting value of R_1 and l, respectively

$\Delta R_1 = R_1 - R_1^*$ = deviation of R_1

$\Delta l = l - l^*$ = deviation of l.

Accordingly, calculated rotor-flux $\boldsymbol{\psi}^c$ is represented in (18):

$$\boldsymbol{\psi}^c = \frac{T_L}{1 + T_L p} \cdot \boldsymbol{e}^c + \frac{1}{1 + T_L p} \cdot \boldsymbol{\psi}^* \tag{18}$$

where T_L is the time constant of the lag circuit.

Particularly, in a steady state, (18) can be rewritten as

$$\boldsymbol{\psi}^c = \frac{T_L}{1 + j\omega T_L} \cdot \boldsymbol{e}^c + \frac{1}{1 + j\omega T_L} \cdot \boldsymbol{\psi}^*. \tag{19}$$

Putting $\boldsymbol{e} = j\omega\boldsymbol{\psi}$, $p\boldsymbol{i}_1 = j\omega\boldsymbol{i}_1$, and

$$\frac{1}{1 + j\omega T_L} = \frac{1}{\{1 + (\omega T_L)^2\}^{1/2}} \cdot \epsilon^{-j\gamma_c} = F_L$$

where $\gamma_c = \tan^{-1}(\omega T_L)$, (19) can be rewritten as follows:

$$\begin{aligned} \boldsymbol{\psi}^c &= \boldsymbol{\psi} + F_L(\boldsymbol{\psi} - \boldsymbol{\psi}^*) \\ &\quad + (T_L \Delta R_1 - \Delta l) F_L \boldsymbol{i}_1 + \Delta l \boldsymbol{i}_1 \end{aligned} \tag{20}$$

where $\Psi = MI_1 \cos\gamma$, $\Psi^* = M^* I_1 \cos\gamma^* = M^* I_{d1}^*$, $\gamma^* = \tan^{-1}(\omega_s^* T_2)$, $\gamma = \tan^{-1}(\omega T_2)$, and $\gamma_c = \tan^{-1}(\omega T_L)$.

Refer to Fig. 4 for a better understanding of (18)–(20). The aforementioned method is compared with the conventional method on a vector diagram.

A. Conventional Method – No Existence of ψ^*

Even if motor parameter errors are negligible, phase error $\delta_c = \tan^{-1}(1/\omega T_L)$ with the lag-circuit remains. In addition, the larger the T_L, the better performance of the estimated rotor-flux vector, but it is limited actually by the integrator thermal drift, and so on.

B. Proposed Method – Existence of ψ^*

Phase error δ_c with the lag circuit can be approximately compensated by the component of ψ^*, and the error components of motor parameters remain. Consequently, resultant phase error δ_u of the calculated rotor flux in the conventional method is changed to resultant phase error δ_p in the proposed method, and, therefore, the calculation of the rotor flux can be established at a very low frequency in the proposed method. Because the rotor-flux vector at standstill and $I_{q1} = 0$ agree with the current vector due to the dc-exciting current, the rotor flux coincides with the command of the exciting current. Accordingly, the initial value of the rotor-flux estimator can be set by the command of the rotor flux.

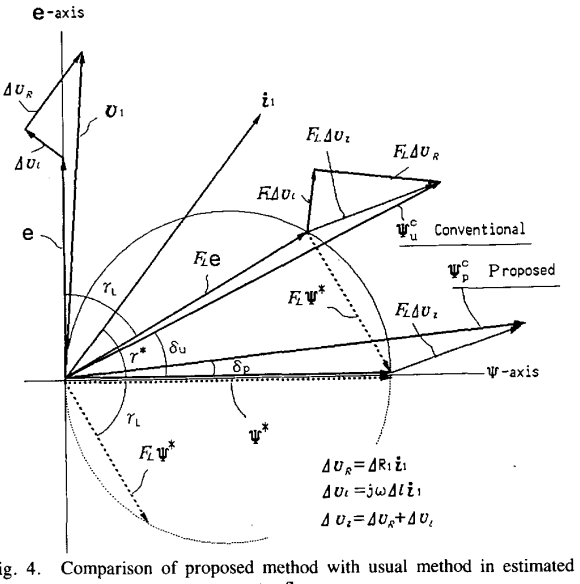

Fig. 4. Comparison of proposed method with usual method in estimated rotor flux.

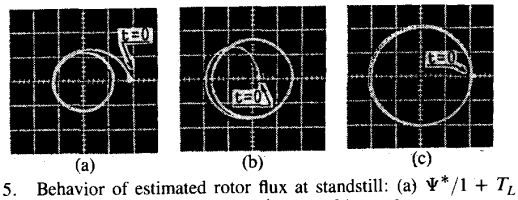

Fig. 5. Behavior of estimated rotor flux at standstill: (a) $\Psi^*/1 + T_L$; (b) $T_L e^c/1 + T_L$; (c) $\Psi^* + T_L e^c/1 + T_L$.

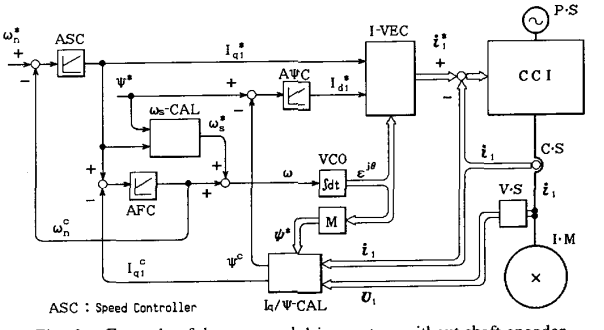

Fig. 6. Example of the proposed drive system without shaft encoder.

Fig. 5 shows the behavior of the rotor-flux vector in the proposed rotor-flux estimator, which was tested in a step change of the torque command at standstill. As a result, the resultant rotor flux (Fig. 5(c)) had no transient in spite of the

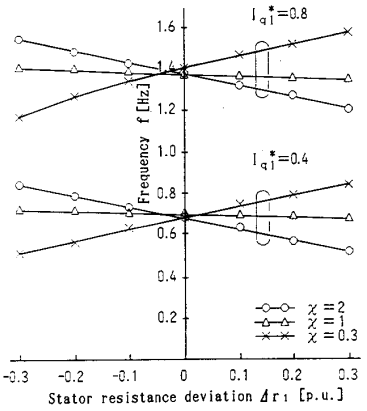

Fig. 7. Relation between stator-resistance variation and operating frequency at standstill.

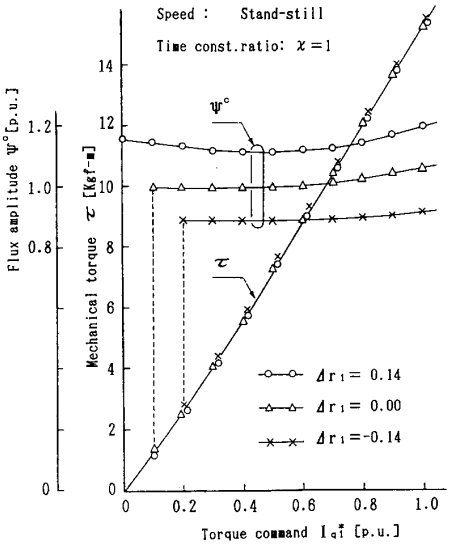

Fig. 8. Torque characteristics at standstill.

TABLE I
MOTOR RATING AND PARAMETERS

Name Plate Rating: 30 kW, 1800 r/min, Four Poles	
Stator voltages, rms	135V
Magnetizing current, rms	47 A
Torque current, rms	131 A
Stator resistance, $\%R_1$	1.95%
Rotor resistance, $\%R_2$	2.18%
Mutual reactance, $\%X_m$	295%
Total leakage reactance, $\%X_1$	17.1%
Rotor time constant, T_2	0.25 s

existing transient on both the rotor-induced voltage (Fig. 5(a)) and the rotor-flux command (Fig. 5(b)).

Next, the influence of motor parameters, particularly a resistive parameter such as the third term in (20), is studied. The third term of (20) is as rewritten as follows:

$$(T_L\Delta R_1 - \Delta l)F_L i_1 = .(T_L\Delta R_1 - \Delta l)F_L i_{d1}^* \epsilon^{j(\gamma^* - \gamma_c)}. \quad (21)$$

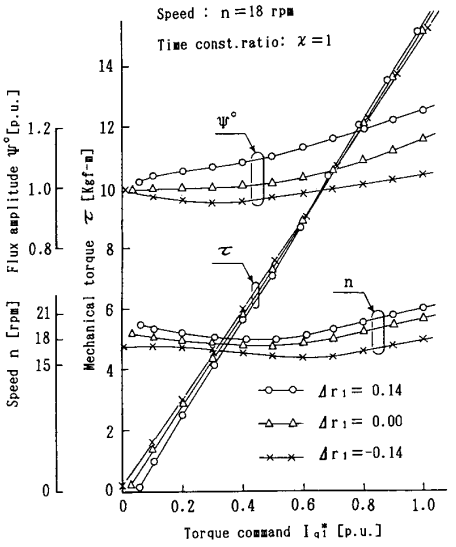

Fig. 9. Torque and speed characteristics at low speed.

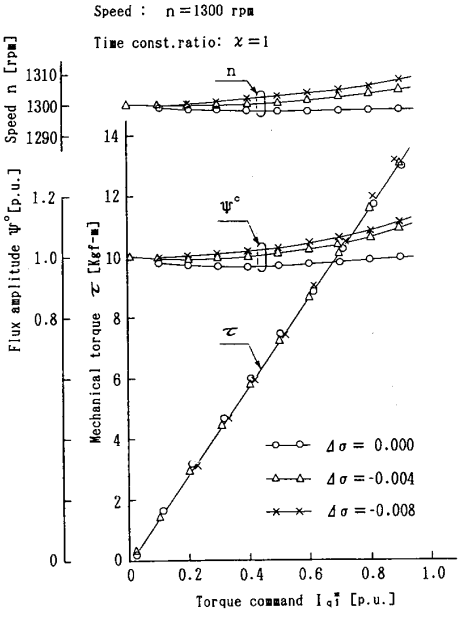

Fig. 10. Torque and speed characteristics at moderate speed.

The phase error to the rotor-flux command axis is examined by $\gamma^* - \gamma_c$. where $\gamma^* = \tan^{-1}(\omega_s^* T_2)$, $\gamma_c = \tan^{-1}(\omega T_L)$, $\omega = \omega_n^c + \omega_s^*$, and $\omega = \omega_s$ at standstill.

When T_L is assumed to be equal to T_2, $(\gamma^* - \gamma_c)$ becomes zero at standstill. Consequently, when $T_L = T_2$, the phase error caused from the resistive parameters is reduced to a smaller level, at low speed or almost standstill.

IV. EXPERIMENTAL SYSTEM AND RESULTS

Fig. 6 is a configuration of the proposed system, which consists of a digital controller and calculator, an analog controller, a current-controlled PWM transistor inverter, and

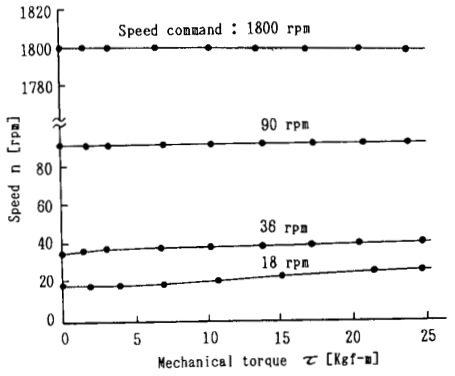

Fig. 11. Torque-speed characteristics.

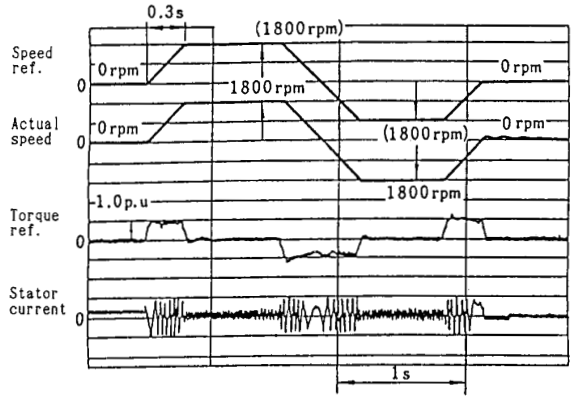

Fig. 12. Speed response for reversible change in speed reference.

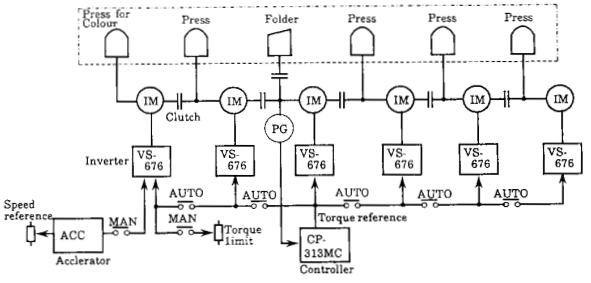

Fig. 13. Configuration of drive system employed for a rotary press. AUTO = interconnecting drive mode; MAN = individual drive mode; IM = squirrel-cage induction motor; VS-676 = vector-control inverter without shaft encoder; CP-313MC = programmable controller; PG = common pulse generator at interconnecting drive mode.

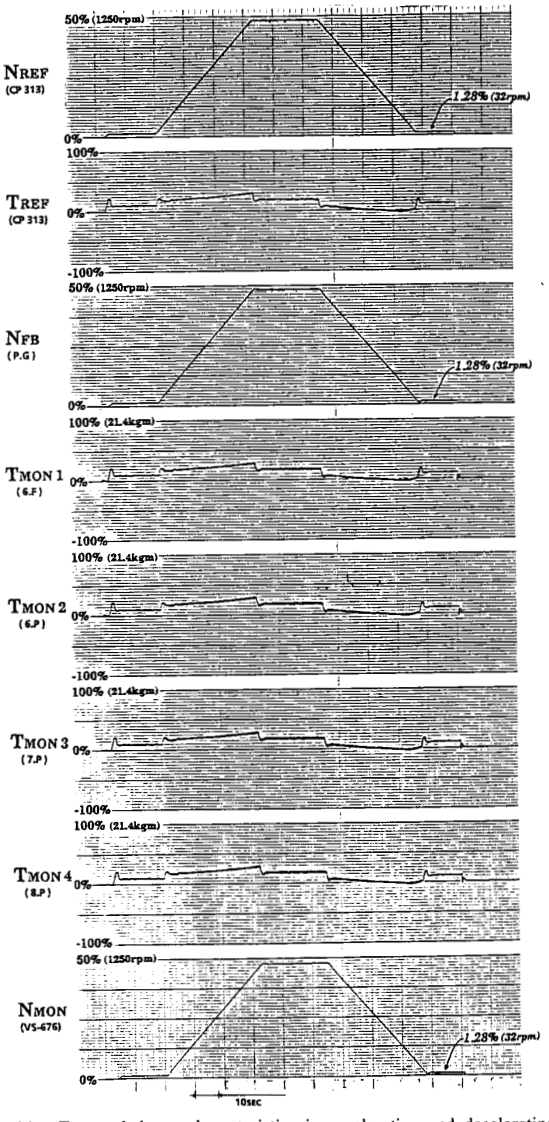

Fig. 14. Torque balance characteristics in accelerating and decelerating. N_{REF} = speed reference; T_{REF} = torque reference; N_{FB} = speed actual value; $T_{MON1,2,3,4}$ = torque monitor; N_{MON}.

a 30-kW nominal-rated squirrel-cage induction motor, using the scheme stated in Sections II and III. The system was estimated with a torque meter and a speed sensor coupled with the motor shaft, respectively, as a reference of the desired level. Table I shows the rating and parameters of the applied motor.

Speed control is carried out using an estimated speed signal ω_n^c, which is calculated from rotor-flux speed ω and slip speed command ω_s^*. Whereas an addition of signal ω_s^* and the output signal of AFC is imposed to input of VCO, the output signal of AFC, therefore, is equivalent to the speed signal ω_n^c.

The flux-control loop acts only at a moderate speed and does not act in a low speed. The results of several tests in the proposed system can be seen in Figs. 7–12. Fig. 7 shows the influence of the stator-resistance variation $\Delta r_1 = \Delta R_1 / R_1^*$ at standstill in relation to time constant ratio $x = T_L / T_2$. The result indicates that the operating frequency was controlled constantly with respect to the stator-resistance variation, if we assume that $x = 1$. In other words, the operating frequency was independent of the stator-resistance variation.

Fig. 8 shows the characteristics of the shaft torque and the calculated rotor flux for the stator-resistance variation at standstill. As a result, although the calculated rotor flux

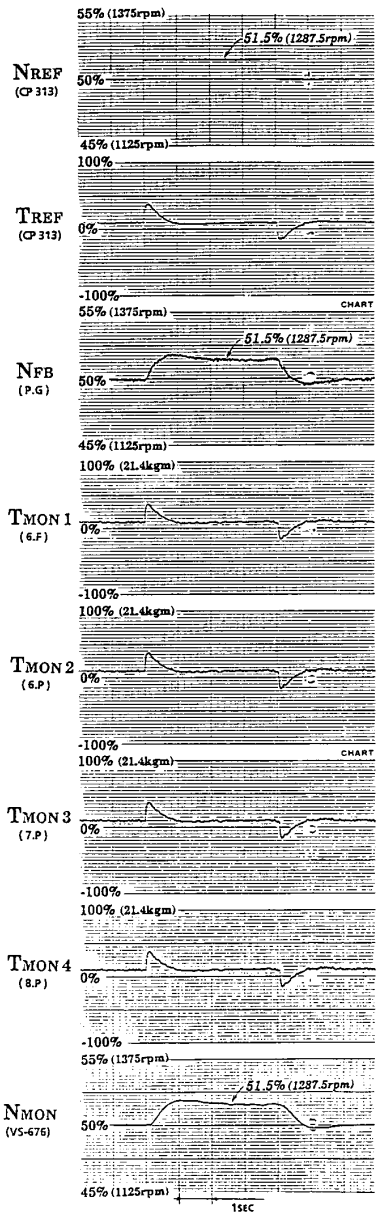

Fig. 15. Torque balance characteristics in step change of speed. N_{REF} = speed references; T_{REF} = torque reference; N_{FB} = speed actual value; $T_{MON1,2,3,4}$ = torque monitor; N_{MON}.

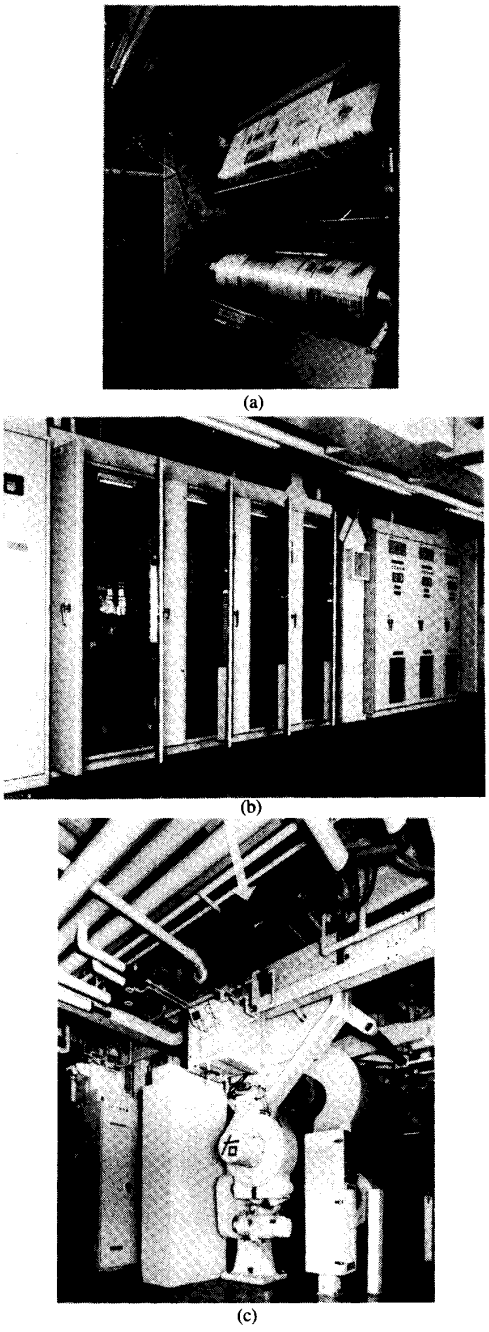

(a)

(b)

(c)

Fig. 16. General view of rotary offset press and electrical equipment: (a) Rotary offset press in printing operation; (b) switchgear cubicle with vector control inverter VS-676; (c) drive motor interconnected on a common shaft above the reel-changer unit.

varied greatly, the torque was found to be independent of the stator resistance and to have a good linearity.

Fig. 9 shows characteristics of the torque and speed at a very low speed. As a result, the system had good performance, even at 1/100 of the rated speed.

Fig. 10 shows characteristics of the torque and speed at relatively high speed, for leakage-inductance variation $\Delta\sigma = \Delta l/M^*$, indicating that the system had good performance in spite of little speed variation.

Fig. 11 shows the performance of the speed control that was obtained by using the calculated speed signal at the various speed commands. The result indicates that the system had good accuracy speed from 1.0% to the rated speed.

Although no speed sensor was provided, a reasonable relation between torque and speed was obtained in the proposed method under 18–1800 r/min, and the system was well controlled even at standstill.

Fig. 12 shows the dynamic behavior in the reversible

operation from forward top speed to reverse top speed. As a result, the system has a good performance as dc motor.

V. Application for Printing Presses

Most rotary offset presses in Japan are driven by dc motors that have outstanding features on smooth speed control during printing. However, they require very careful maintenance for stable operations. Thanks to development of inverter technologies, ac motors have been recently used in the field of offset presses without any problems in Japan.

Fig. 13 shows the configuration of a drive system employed on rotary offset presses. It has two kinds of operations, one for individual operation without shaft encoder for setting printing plates and one for interconnecting operation with a common shaft encoder for normal printing works.

For the rotor presses, the following requirements should be satisfied:

1) *Torque stability control for common shaft drives:* The control system should be designed flexibly to meet selected presses concerning printing pages or colors. Torque balance level is seen in Fig. 14 when four motors are driven in an interconnecting operation.
2) *Wide speed control range in excess of 1:100:* In case of individual operation, precise positioning control is required.
3) *High accuracy of speed control in interconnecting operations:* The required speed stability of $\pm 0.1\%$ of rated speed to keep desired web tension is maintained under all operating conditions. These requirements were accomplished by the proposed ac drive system.

Fig. 14 shows the torque balance level during accelerating and decelerating among 0, 32, and 2500 r/min when four motors are driven in interconnecting operations.

Fig. 15 shows the quick response of the speed at the same points of measuring in Fig. 14. The results indicate that both the speed response and the torque balance had good performance for the request of the rotary presses.

Fig. 16 shows a rotary offset press in printing operation, a switchgear cubicle with vector-control inverter VS-676, and drive motor interconnected on a common shaft above the reel-changer unit.

This new drive system, furthermore, is available for various industrial fields that have harmful surroundings (i.e., high temperature, high humidity, vibration, etc.) and enables optimum application, especially in a common shaft drive system with several motors.

VI. Conclusions

A novel method of torque control in induction motors is proposed, which is independent of motor parameters and requires no sensor for the motor.

These features have been verified by experimental results implementing 30-kW PWM inverter and motor systems. The main results obtained in this paper are as follows:

1) Performance of torque control does not depend on both rotor resistance and stator resistance.
2) At standstill, the system is controllable in terms of the proposed flux estimator.
3) Even if a speed sensor is not provided, speed control is possible with good accuracy.

We are confident that these approaches solve the problems of high-quality torque and speed control using induction motors without a shaft sensor.

References

[1] T. Ohtani, "Torque control using the flux derived from magnetic energy in induction motors driven by static converter," in *Conf. Rec. IPEC-Tokyo '83*, pp. 696-707.
[2] T. Ohtani *et al.*, "Parameter adaption for vector controlled induction motor drives," *Yaskawa Denki*, vol. 181, pp. 232-238, 1983.
[3] M. P. Kazmierkowski and H. Kopcke, "A simple control system for current source induction motor drives," *IEEE Trans. Industry Applications*, vol. IA-21, no. 4, pp. 617-623, May/June 1985.
[4] T. Ohtani, "A new method of torque control free from motor parameter variation in induction motor drives," in *Conf. Rec. 1986 Ann. Mtg. IEEE-IAS* (Denver), pp. 203-209.
[5] T. Ohtani *et al.*, "Induction motor drives without speed sensor by vector control," *T. IEEE Japan*, vol. 107-D, no. 2, pp. 199-206, 1987.
[6] T. Ohtani *et al.*, "Vector control of induction motors without speed sensors," *Yaskawa Denki*, vol. 195, pp. 81-88, 1987.
[7] X. Xu, R. De Doncker, and D. W. Novotony, "A stator flux oriented induction machine drive," in *Proc. IEEE-PESC '88* (Kyoto, Japan), Apr. 1988, pp. 870-876.
[8] —, "Stator flux orientation induction machines in the field weakening region," in *Conf. Rec. IEEE/IAS Ann. Mtg.* (Pittsburgh, PA), Oct. 1988, pp. 437-443.
[9] R. De Doncker and D. W. Novotony, "The universal field oriented controller," in *Conf. Rec. IEEE/IAS Ann. Mtg.*, (Pittsburgh, PA), Oct. 1988, pp. 450-456.

Tsugutoshi Ohtani (M'91) was born in Kumamoto Prefecture, Japan, in 1939. He received the B.E. degree from Kumamoto University, Japan, in 1962. He received the Dr.Eng. degree from Kyushu University, Japan, in 1991.

Since 1962, he has been developing the area of ac motor adjustable-speed drives including the high-performance vector control of induction motors at the Research Laboratory and Yukuhashi Plant of the Yaskawa Electric Mfg. Co., Ltd. Presently, he is technical manager at Inverter Division, Yukuhashi Plant.

Dr. Ohtani is a member of the Institute of Electrical Engineers of Japan.

Noriyuki Takada was born in Saga Prefecture, Japan, in 1953. He received the B.E. degree from Kyushu University, Japan, in 1977.

Since 1977, he has been engaged in the development and design of adjustable-speed drives at Yaskawa Electric Mfg. Co., Ltd. He was transferred to the Yaskawa Electric America in 1989 and is presently the Chief Application Engineer of Drives and Systems Division.

Koji Tanaka was born in Kagoshima Prefecture, Japan, in 1945. He received the B.S. degree in electrical engineering from Kanazawa University, Japan, in 1968.

He joined Yaskawa Electric Manufacturing Company, Ltd in 1968. Since then, he has been engaged in the system application design of adjustable-speed drives. Presently, he is a Manager of Industrial Drives Engineering at the System Plant of Yaskawa Electric Mfg. Co., Ltd.